

MAGNET/CRYOCOOLER INTEGRATION FOR THERMAL STABILITY IN CONDUCTION-COOLED SYSTEMS

H.-M. Chang and K.B. Kwon

Department of Mechanical Engineering, Hong Ik University
Seoul, 121-791, Korea

ABSTRACT

The stability conditions that take into accounts the size of superconducting magnets and the refrigeration capacity of cryocoolers are investigated for the conduction-cooled systems without liquid cryogens. The worst scenario in the superconducting systems is that the heat generation in the resistive state exceeds the refrigeration, causing a rise in the temperature of the magnet winding and leading to burnout. It is shown by an analytical solution that in the continuously resistive state, the temperature may increase indefinitely or a stable steady state may be reached, depending upon the relative size of the magnet with respect to the refrigeration capacity of the cryocooler. The stability criteria include the temperature-dependent properties of the magnet materials and the refrigeration characteristics of the cryocooler. A useful graphical scheme is presented and the design of the stable magnet /cryocooler interface is demonstrated.

INTRODUCTION

Conduction-cooling with a closed-cycle refrigerator is an excellent option for relatively small superconducting systems. Since no liquid cryogens are necessary, the systems are easier to operate and more compact in structure than the conventional liquid-cooled systems. In addition, the conduction-cooled systems are more efficient with respect to energy consumption, mainly because the thermal loss associated with the storage and the transfer of cryogenic liquids is obviated. Conduction-cooling is effective especially for HTS magnets [1-4] whose operating temperature is in 30-50 K range, since no pure substance can exist as liquid in this range.

On the other hand, some new difficulties have arisen in the development of liquid-free systems, one of which is to secure the stability of the magnet for any thermal disturbance. Because of its practical importance, many researchers have investigated the HTS stability problem for the past several years[4-8]. Most of the investigations have been focused on quench behavior and propagation of the normal zone by incorporating the temperature-dependent properties of the magnet materials. In order to exploit the stability of the

conduction-cooled HTS magnet, the refrigeration characteristics of the cryocooler should be included as well.

When the high temperature superconductor becomes normal for any reason, the magnet temperature will rise because of the heat generated by electrical resistance. As the temperature increases, the cryocooler is also capable of absorbing more heat from the magnet. Therefore, depending upon the relative magnitude of the heat generation and the refrigeration, the magnet temperature may not rise indefinitely even in the fully resistive state. A similar stability of the uncooled segment of HTS exposed from liquid level has been treated earlier by Dresner[8], but this problem is different because the ends are not clamped at the saturated temperature of the liquid cryogen. As a first step in the study of the magnet/cryocooler integration issue, this paper demonstrates the existence and a stability of steady state for the worst situation in which the HTS magnet continues to be normal.

ANALYSIS

FIGURE 1 shows a typical structure of a superconducting magnet that is conduction-cooled by a two-stage cryocooler. The second stage of the cryocooler is connected thermally to one axial end of the magnet so that the main direction of the heat flow is along the axis of the magnet. It is assumed in this paper that the heat leak to the magnet surface in vacuum is negligible and the heat conduction in the magnet is one-dimensional.

The magnet to be considered in this paper is a pancake, the typical cross-section of which is schematically shown in FIGURE 2. The superconducting composite tapes are made of HTS(subscript B) and metal(subscript A), as in BSCCO/Ag. The volume fraction of metal (A) in the composite (A+B) is defined as f , and it is assumed for simplicity that the cross-section of HTS is a rectangle and has the same aspect ratio as the tape. The composite tapes are wound on a bobbin (subscript G), which is mostly made of G-10. The symbol g is defined as the ratio of the axial length wound by the HTS composite tape to the total length of the pancake.

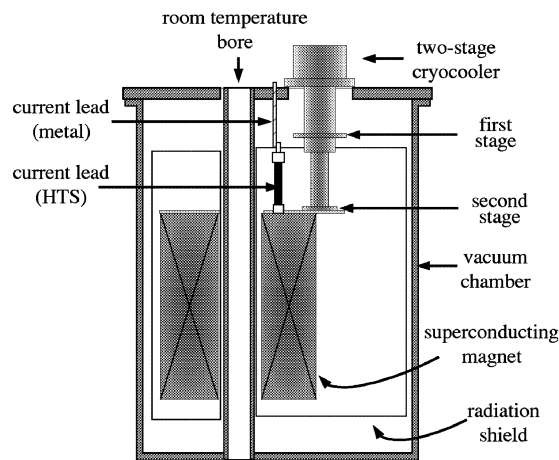


FIGURE 1. Structure of a typical superconducting magnet conduction-cooled by a two-stage cryocooler.

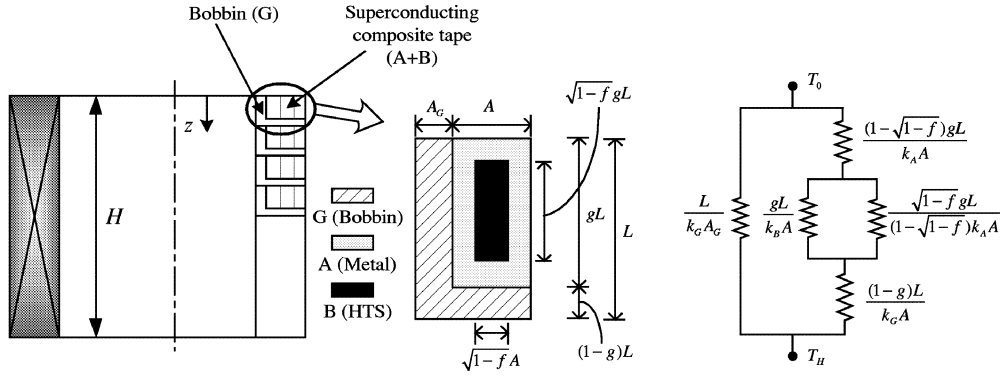


FIGURE 2. Schematic cross-section of a pancake and thermal resistance circuit for composite conductor.

Steady-State Temperature and Heat Generation

The steady-state temperature, $T(z)$, of the pancake magnet is determined by the heat conduction equation

$$\frac{d}{dz} \left(k(T) \frac{dT}{dz} \right) + \frac{g}{f} \cdot \rho_A(T) \cdot J^2 \cdot G(T) = 0 \quad (1)$$

where the magnet is considered as a homogeneous medium having an equivalent (or averaged) thermal conductivity $k(T)$. $\rho_A(T)$ is the temperature-dependent electrical resistivity of the metal and J is the current density in the HTS composite tape. $G(T)$ is the so-called current-sharing function that is defined as the fraction of the current flowing in the metal. In this analysis, $G(T)$ is set to 1, since the normal resistive state is considered. The axial coordinate, z , is the distance from the cold end that is connected to the cryocooler.

The equivalent conductivity, $k(T)$, is calculated from the corresponding thermal resistance circuit shown in FIGURE 2. In a practical case in which the metal has a much greater thermal conductivity than the HTS and the bobbin material, i.e. $k_A \gg k_B$ and $k_A \gg k_G$, $k(T)$ can be simplified to

$$\frac{1}{k(T)} \approx \left(\frac{2 - \sqrt{1-f} - f}{1 - \sqrt{1-f}} \right) \frac{g}{k_A(T)} + \frac{(1-g)}{k_C(T)} \quad (2)$$

The boundary conditions for equation (1) are given by

$$T(0) = T_0, \quad \frac{dT(H)}{dz} = 0 \quad (3)$$

where the cold end temperature, T_0 , is not a fixed value, but determined by the cooling rate of the cryocooler. In the second boundary condition, the radiation heat transfer on the bottom surface has been neglected.

In order to derive a general expression for the heat generation in the magnet, equation (1) is first multiplied by $k(T)$

$$k(T) \frac{dT}{dz} \cdot \frac{d}{dT} \left(k(T) \frac{dT}{dz} \right) = -\frac{g}{f} \cdot k(T) \cdot \rho_A(T) \cdot J^2 \quad (4)$$

which can be integrated from an arbitrary T to T_H , where $T_H = T(H)$,

$$\frac{1}{2} \left(k(T) \frac{dT}{dz} \right)^2 = \frac{g}{f} \cdot J^2 \int_T^{T_H} k(\tau) \rho_A(\tau) d\tau \quad (5)$$

In the integration, the boundary condition at $z = H$ has been applied. By the method of separation of variables, equation (5) is rearranged and integrated again from $z = 0$ to H or from $T = T_0$ to T_H , to obtain the relation between the two end temperatures of the magnet in steady state

$$\int_{T_0}^{T_H} \frac{k(T) dT}{\sqrt{\int_T^{T_H} k(\tau) \rho_A(\tau) d\tau}} = J \sqrt{\frac{2g}{f}} \cdot H \quad (6)$$

The right hand side of equation (6) does not include any temperature-dependent properties. The heat flux at $z = 0$ can be derived directly by integrating the square-root of equation (5) from $z = 0$ to H or from $T = T_0$ to T_H . The total heat generated in the resistive magnet is identical to the heat transfer rate at $z = 0$ in the steady state

$$Q_{heat} = k(T_0) A \frac{dT(0)}{dz} = J \cdot A \sqrt{\frac{2g}{f} \int_{T_0}^{T_H} k(\tau) \rho_A(\tau) d\tau} \quad (7)$$

where A is the cross-section area of the magnet in the axial direction.

Equations (6) and (7) are general expressions for calculating the heat generation rate, Q_{heat} , as a function of the cold end temperature T_0 . Once T_0 is given, the warm end temperature, T_H , is calculated from equation (6), with the given dimensions, the materials, and the current density of the magnet. The two end temperatures are then substituted into equation (7) to yield Q_{heat} .

The general expressions can be greatly reduced if the temperature-dependent properties are given by simple functions. For the metal in the HTS composite tape, such as silver, the Wiedemann-Franz law can be satisfactorily applied as given by

$$k_A(T) \rho_A(T) = L_0 T \quad (L_0 = 2.45 \times 10^{-8} V^2/K^2) \quad (8)$$

Furthermore, $\rho_A(T)$ can be taken as a power function of T over a certain range

$$\rho_A(T) = \rho_{LN} \left(\frac{T}{T_{LN}} \right)^n \quad (9)$$

where the subscript LN indicates the reference values at liquid-nitrogen temperature. In the temperature range 77-300 K, n has a value between 1 and 1.5 for silver[8]. If n is taken to be 1 for simplicity, $k_A(T)$ is a constant from equation (8). The thermal

conductivity of bobbin material, such as G-10, does not vary significantly with temperature in this range, so $k(T)$ may well be assumed to be a constant from equation (3). Integration in equations (6) and (7) can be performed to yield

$$\frac{T_0}{T_H} = \cos \left(\sqrt{\frac{g \cdot L_0}{f \cdot k \cdot k_A}} J \cdot H \right) \quad (10)$$

$$Q_{heat}(T_0) = \sqrt{\frac{g \cdot k \cdot L_0}{f \cdot k_A}} J \cdot A \cdot T_0 \cdot \tan \left(\sqrt{\frac{g \cdot L_0}{f \cdot k \cdot k_A}} J \cdot H \right) \quad (11)$$

It is carefully noted in equation (11) that the heat generation in the magnet is proportional to T_0 and the proportional constant is associated with the dimensions (A, H, g, f), the materials (k_G, k_A), and the current density (J) of the magnet. In order for Q_{heat} to have a finite value,

$$\sqrt{\frac{g \cdot L_0}{f \cdot k \cdot k_A}} J \cdot H < \frac{\pi}{2} \quad (12)$$

which is the same stability condition for a segment of the conductor exposed from liquid cryogen, as Dresner presented earlier[8].

Refrigeration by Cryocooler

The refrigeration capacity of any cryocooler increases as the refrigeration temperature increases. The detailed characteristics of the cryocooler, however, may vary widely depending upon the thermodynamic cycle, the size, the operating conditions, the manufacturer, and so on[9]. For the purpose of a quantitative discussion in this paper, we assume a reasonable functional relation between the refrigeration capacity and the cold end temperature as

$$Q_{ref}(T_0) = Q_{LN} \frac{\ln T_0 / T_b}{\ln T_{LN} / T_b} \quad (13)$$

where T_b is the lowest (or base) temperature obtained when no heat is generated in the magnet and Q_{LN} is the refrigeration capacity at liquid-nitrogen temperature T_{LN} .

RESULTS AND DISCUSSION

Stability Condition

As demonstrated in the previous sections, both the heat generation in the magnet and the refrigeration by the cryocooler increase as the temperature increases. The existence of a steady state is determined by the relative magnitude of the two quantities. The refrigeration capacity and the heat generation rate are calculated as functions of the cold end temperature from equations (11) and (13), respectively, and plotted in FIGURE 3. The specifications of the magnet used in the calculation are listed in TABLE 1.

TABLE 1. Specifications of Pancake Magnet in the Sample Calculation

Magnet Shape	Volume Fraction of Metal(A) in HTS Tape(A+B)	f	0.7
	Axial Length Fraction of Tape(A+B) in Pancake Magnet	g	0.9
	Coil Inner Diameter		0.10 m
	Coil Outer Diameter		0.15 m
Operation	Current Density	J	$3.5 \times 10^6 \text{ A/m}^2$
Cryocooler	Refrigeration Capacity at $T_{LN} = 77\text{K}$	Q_{LN}	80 W
	Operation Temperature	T_b	40 K
Materials	Electrical Resistivity of Silver(A) at $T_{LN} = 77\text{K}$	ρ_{LN}	$2.09 \times 10^{-9} \Omega \cdot m$
	Thermal Conductivity of G-10(G)	k_G	$0.7 \text{ W/m} \cdot \text{K}$

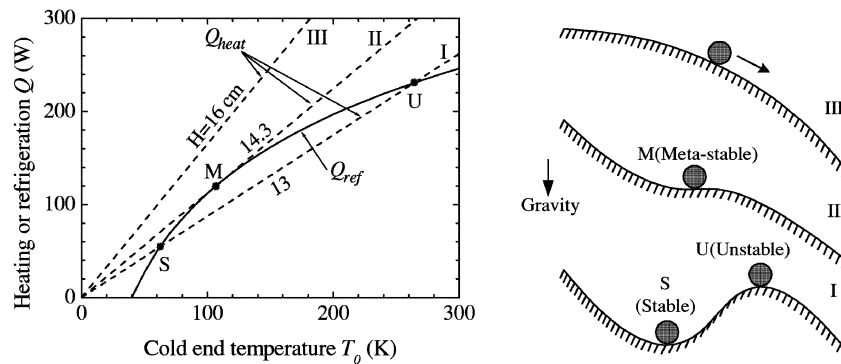


FIGURE 3. Heat generation and refrigeration capacity as functions of temperature to demonstrate the existence and the stability of steady-state.

The three dashed lines in FIGURE 3 represent the heat generation for three different values of magnet height. In Case I, the magnet is relatively short so that the heat generation line has a relatively small slope and intersects the refrigeration curve at two points, S and U. It means that two steady states are possible, but only one (S) of them is the stable steady state; the other (U) is unstable. If T_0 is smaller than the temperature at S, the heat generation exceeds the refrigeration, so the temperature will increase to move toward S. On the contrary, when T_0 has a value between S and U, the refrigeration exceeds the heat generation, and the temperature will decrease to move toward S again. If T_0 is greater than the temperature at U, however, the temperature will increase indefinitely. The stability of the steady states can be compared with that of the curved surfaces in the gravitational field, as shown in FIGURE 3.

In Case II, the magnet height has a marginal value such that there is a unique steady state, indicated by M. The steady state is called metastable, because it can be reached only from the lower temperature region. If the height is even greater than the critical value in Case II, the heat generation always exceeds the refrigeration and the steady state will never be reached, which is represented by Case III.

The condition for the conduction-cooled magnet to have a stable or at least a metastable steady state is generally given by

$$Q_{heat}(T_0) \leq Q_{ref}(T_0) \quad (14)$$

If equations (11) and (13) are substituted into the two functions of equation (14), the stability condition of the pancake magnet can be written as

$$\sqrt{\frac{g \cdot k \cdot L_0}{f \cdot k_A}} J \cdot A \cdot T_0 \cdot \tan\left(\sqrt{\frac{g \cdot L_0}{f \cdot k \cdot k_A}} J \cdot H\right) \leq Q_{LN} \frac{\ln T_0 / T_b}{\ln T_{LN} / T_b} \quad (15)$$

As discussed in the previous paragraph, there exists a maximum height below which the magnet has a steady state, which can be expressed by rearranging equation (15)

$$H \leq H_{\max} = \sqrt{\frac{f \cdot k \cdot k_A}{g \cdot L_0}} \frac{1}{J} \cdot \tan^{-1}\left(\sqrt{\frac{f \cdot k_A}{g \cdot k \cdot L_0}} \frac{Q_{LN}}{e \cdot A \cdot J \cdot T_b \ln\left(\frac{T_{LN}}{T_b}\right)}\right) \quad (16)$$

where e is the base of the natural logarithm.

Magnet Design for Stability

It is worthwhile to examine the effect of significant design parameters on the thermal stability of the conduction-cooled magnet. All the data in this section have been generated for the conditions listed in TABLE 1, unless mentioned otherwise.

FIGURE 4 shows the maximum height needed to assure the stability as a function of the refrigeration capacity of the cryocooler, for various values of the operating current density. H_{\max} is nearly proportional to Q_{LN} , for relatively small Q_{LN} 's, but approaches asymptotically to a constant value even when Q_{LN} gets very large. It means that a larger magnet can be cooled with stability to a certain extent when a cryocooler with larger capacity is employed. The refrigeration capacity, however, cannot ensure the stability of the excessively oversized magnet. It should be noted that the effect of the current density is even more significant in stability issue. As the current density increases, the size of the magnet needs to be reduced dramatically for thermal stability to be achieved.

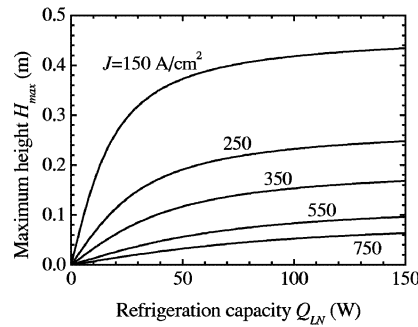


FIGURE 4. Maximum height of magnet as a function of refrigeration capacity for various values of current density

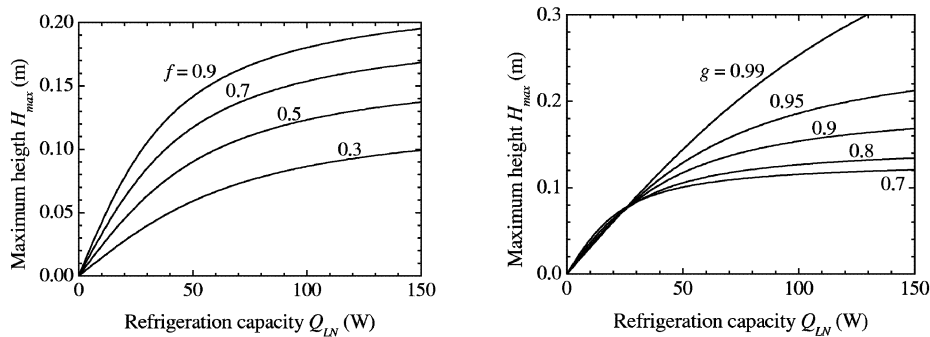


FIGURE 5. Maximum height of magnet as a function of refrigeration capacity for various values of volume fraction of silver (f) and length fraction of HTS tape (g).

FIGURE 5 shows the effect of the volume fraction of silver in the BSCCO tape, f , and the axial length fraction of the tape in the pancake, g . It can be generally stated that a better thermal stability can be expected with smaller values of f and g . In practice, the variation of f is quite limited due to the fabrication process of the HTS composite tape. The second graph of FIGURE 5 suggests that a very small axial thickness of bobbin and a large capacity of cryocooler can be quite effective in improving the thermal stability.

CONCLUSIONS

A concise analytical condition for the thermal stability of a conduction-cooled magnet is derived. The condition expresses how the material properties, the operating current, the dimensions of the magnet and the refrigeration capacity of the cryocooler should be related in order for the magnet to have at least a steady state when the HTS becomes normal. While the quantitative results are obtained only for simplified models, describing the temperature dependence of the properties and the cryocooler performance, the same method can be expected to lead to a more realistic stability condition if more accurate models are incorporated.

REFERENCES

1. Hase, T. et al., *Cryogenics* **38**, pp. 971-977 (1998).
2. Daugherty, M.A. et al., "Ramp Rate Testing of an HTS Gradient Magnetic Separation Magnet," in *Advances in Cryogenic Engineering* 43A, edited by P. Kittel, Plenum, New York, 1998, pp. 165-171.
3. Lee, H.J. et al., *J. Korea Institute of Applied Superconductivity and Cryogenics* **2**, pp. 37-43 (2000).
4. Lim, H. and Iwasa, Y., *Cryogenics* **37**, pp. 789-797 (1997).
5. Lue, J.W. et al., "Quench Development in a High Temperature Superconducting Tape," in *Advances in Cryogenic Engineering* 41A, edited by P. Kittel, Plenum, New York, 1996, pp. 433-440.
6. Dresner, L., *Stability of Superconductors*, Plenum, New York, 1995, pp. 53-127.
7. Dresner, L., *Cryogenics* **33**, pp. 900-909 (1993).
8. Dresner, L., "Stability of an Uncooled Segment of a High-Temperature Superconductors," in *Advances in Cryogenic Engineering* 39A, edited by Kittel, P., Plenum, New York, 1994, pp. 429-435.
9. Chang, H.M. and Van Sciver, S.W., "Optimal Integration of Binary Current Lead and Cryocooler," *Cryocoolers* 10, edited by Ross, R.G., Plenum, New York, 1999, pp. 707-716.